university of groningen / faculty of science and engineering

Bachelor's Thesis

A comparison of laser absorption spectrometry with Isotope Ratio Mass Spectroscopy in determining isotopic composition of reference materials.

Author:
Kaushalkumar Chaniyara
S3614603

Supervisors:
prof H.A.J Meijer
prof R.A Hoekstra
Daily Supervisors:
P.M Steur
dr. ir. H.A.Scheeren

1 Abstract

This research is aimed at making a comparison between a number of data analysis methods to measure the values of δ^{13} and δ^{18} in Carbon Dioxide for the SICAS. Consequently, a comparison against the IRMS is carried out for a range of reference calcites used to calibrate measurement devices. The dilution setup used to create the samples is optimized and then tested for reliability and ability to prevent altering of samples.

The results show that the quadratic fit works best when analyzing the data and that the ratio and isotopologue method perform equally well overall. The residual values for δ^{13} and δ^{18} have been shown to be very consistent, leading to the conclusion that deviations from the norm occur mainly due to calibration issues. The IRMS has been proven to have an accuracy equivalent to the SICAS for the purposes of this experiment and the dilution setup has been confirmed to be reliable and prevent contamination of the sample.

Contents

2 Introduction

2.1 Project Overview

Carbon dioxide concentrations have been rising exponentially in the past few decades as the energy consumption per capita has increased substantially. CO_2 concentrations have increased by almost 50% since the pre-industrial levels in 1850 to a current concentration of 417 parts per million(ppm)[1]. The increase has resulted in global warming, disrupting the balance of terrestrial and aquatic ecosystems and its inhabitants due to the increased temperature[2]. As CO_2 is the greenhouse gas with the highest contribution to these factors, it is imperative that we monitor its atmospheric concentration to ensure we can take the necessary precautions to limit its adverse effects[3]. In order to accurately track and predict this increase in the CO_2 concentration, it is important to track two primary factors, the global primary production and terrestrial ecosystem respiration[4]. The net primary production can then be tracked with the help of these two values, and the increase in CO_2 levels can be tracked over a period of time. The reason for tracking this is that the terrestrial biosphere acts as a carbon sink, and is thus very important for calculations of CO_2 concentrations caused by future emissions. As this sink itself is climate dependent, the whole system is characterised by feedback; therefore the details of the system must be understood and quantified.

The global primary production can be measured by analysing the differences in isotopic composition of the oxygen and carbon isotopes that make up CO_2. There is a fixed balance in the ratio between the different isotopes due to the fractionation process, and by determining the change in these ratios, the resulting isotopic composition of atmospheric CO_2 and the influence of these processes on the composition can be determined. This is known as isotope fractionation and can occur due to the mass difference between two isotopes or independently of mass too[5]. Fractionation occurs due to physical processes like diffusion and photosynthesis showing a preference of he lighter isotopes, thus leaving an abundance of the heavier isotopes in the original sample. On a global scale, the rate of absorption of CO_2 by the ecosystem can thus be determined by determining these ratios. The seasonal variations in concentration also need to be taken into account and thus a high measurement precision for isotopic ratios is required to ensure that this occurs. Therefore, carrying out these measurements also allows for differentiation between anthropogenic emissions and the natural flux in the ecosystem. This flux is due to the varying levels of sinks and sources which absorb and emit the gas, and the extremely large scale over which they occur[4]. The scale also causes dilution of these isotopes, meaning that the change in ratio between isotopes is relatively small compared to the change the amount of CO_2. This requires precise and accurate measurements, which are carried out by the following methods.

Traditionally, the method used is Isotope Ratio Mass Spectrometry(IRMS), and for the purpose of this thesis, a comparison between this method and Laser Absorption Spectroscopy will be carried out. The goal of this project is to compare and analyze the findings from the two measurement methods, and will be done using primary reference materials. This includes the dilution process that is necessary to prepare the sample and bring it to an atmospheric concentration from its pure calcite form, and subsequent analysis in determining the influencing factors in the results.

Using the traditional IRMS method to measure the concentration of the isotopologues, CO_2 needs to be extracted from the air sample before being measured, which not only is time-

consuming, but also results in the introduction of random and systematic errors due to difficulties in carrying out the extraction at a high efficiency. Furthermore, determination of the individual isotope concentration of δ^{17} accurately requires advanced techniques available to a select few laboratories, thus making the measurement process more time intensive and expensive. When measuring the data for δ^{18}, it is also evident that there is a much higher variability in the measurements as compared to δ^{13} due to temperature and water exchange issues present when creating a sample from a calcite using acids. Therefore, it is imperative to use methods which minimize the discrepancies in measurements between independent sources, thus providing a more unified measuring technique.

Using the LAS method does just that, and offers a few key advantages, being that it does not take as much time for the measurements to be carried out. This is due to the measurement being carried out directly on a dry whole air sample which eliminates the need to extract CO_2 from it. This in turn also reduces the chances of errors being introduced into the measurements. The spectral region used by the LAS method(mid infra-red) also allows for high sensitivity isotopic measurements to be taken. Finally, the LAS system also uses less power and does not require the usage of high vacuum systems and high purity gases, thus cutting down on the carbon footprint created during conducting research[6].

A disadvantage of using this method comes into play during calibration. The reference samples have been processed with the IRMS demands in mind, which means they need to be diluted with CO_2 free air to allow for the calibration between the LAS and IRMS. The dilution procedure involves cryogenic extraction of the CO_2 sample from the storage container using liquid nitrogen, and a subsequent transfer into the dilution setup in a tube shaped attachment. The volume of the tube is fixed and thus when it is full, it will house a fixed amount of CO_2. The sample is then recombined with air that has been scrubbed of CO_2 and H2O, the latter for the purpose of avoiding further isotope fractionation by diffusion into the water, resulting in a sample which has an atmospheric level concentration of CO_2. The sample is then left undisturbed to allow diffusion and the creation of a homogeneous mixture, after which the measurements can be carried out.

For the purposes of this project, samples from the Amazonian rainforest and reference material to establish the VPDB scale will be used.. The present primary calibration material for the VPDB scale is IAEA-603 marble, from which a pure concentration of CO_2 can be extracted by reaction with an acid[7]. Then, the sample will be diluted to achieve a concentration in ppm which is identical to atmospheric concentration after recombination with CO_2 free air at regulated pressures. This creates a sample that can be used for measurements for LAS. The setup for LAS involves the use of two interband cascade lasers, several mirrors, an optical cell and two detectors[8]. The lasers pass through an optical cell which contains the sample to be measured. The detector then picks up these signals and fits the data collected against known absorption profiles and produces a graph over a range of frequencies[8]. This can then be analysed to determine the fractions of different isotopologues present in the material.

2.2 Carbon cycle

Carbon is one of the most important elements on the planet, laying the foundation for all life on Earth. The formation of complex molecules like DNA would not be possible without carbon , bound as CO_2 in the atmosphere, which is also one of the primary regulators of temperature on the Earth. While the total carbon content on the planet stays the same, the exchange between

its constituent parts is always in flux, allowing for sustenance of the biosphere. This exchange between the land, water and air makes up the carbon cycle. For the purpose of this thesis, the fast carbon cycle is focused on, as it is more directly effected by anthropogenic emissions and the exchange between the biosphere, atmosphere, ocean, sediment and land soil[9]. The slow carbon cycle is mainly concentrated around the tectonic system and the rock cycle, taking millions of years to complete. This is illustrated in the diagram below, where the global primary production can be determined by adding the values of all the sources that input carbon into the cycle, while the net primary production is a measure of the total change between the input and the uptake across all sources and sinks in the system.

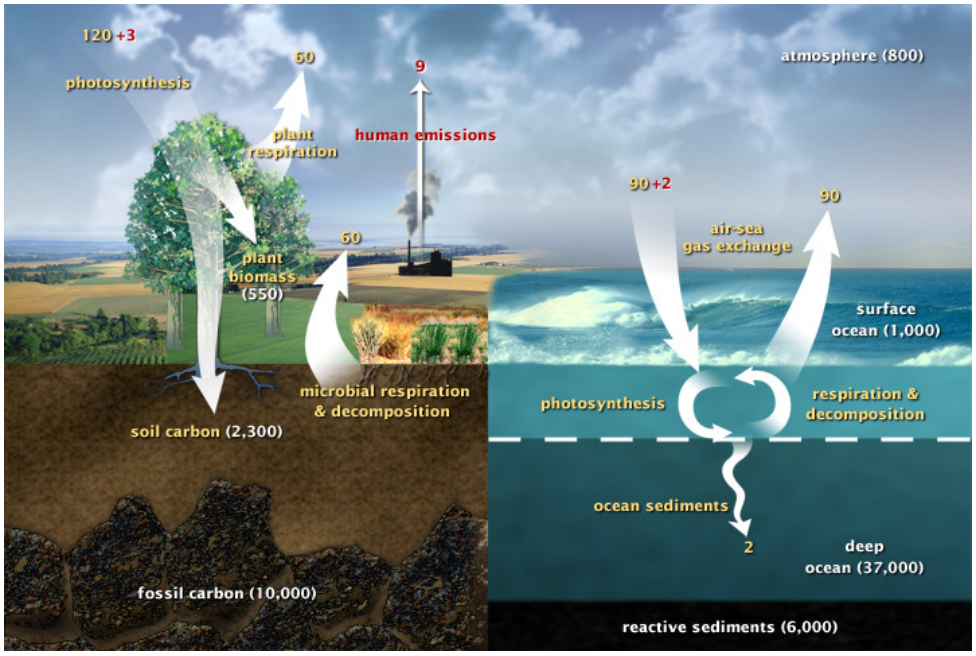

Figure 1: Diagram of the Carbon cycle, with inputs and uptakes given in gigatons per year.[10]

Therefore, the global primary production is essential in helping to determine the increase in concentration of carbon dioxide from anthropogenic emissions and by association can also be used to see how the measures taken to reduce emissions impact the carbon cycle. Due to the nature of the carbon cycle and the process of isotope fractionation, this phenomenon can also be measured by using the isotope ratios of the atoms that make up the carbon dioxide molecule. The ratios of the oxygen and carbon isotopes can then be used to more accurately paint a picture of the carbon cycle in the region and allow for identification of the factors that contribute to the cycle. First the terms used above need to be defined in order to understand the process in more detail.

2.2.1 Isotopes

Isotopes are defined as atoms that have the same number of protons but a different number of neutrons. When these isotopes form a molecule, they create different isotopologues, which are defined by the isotopes that make them up. These isotopologues have different masses due to the differing number of neutrons and thus can be separated and measured. Carbon 13 and Oxygen 18 will be primarily focused on for this research due to their relative abundance and ease of measurement. The method of quantifying the amount of a certain isotope in the atmosphere is

to compare it to a reference standard. Taking carbon 13 as an example, its ratio is compared with the most abundant stable carbon isotope, in this case carbon 12 and then used in the following formula to determine the δ^{13} value of the sample[11]. This provides us with the value in parts per thousand, or per mille.

$$\left(\frac{\frac{13C}{12C}_{sample}}{\frac{13C}{12C}_{reference}} - 1 \right) * 1000 \tag{1}$$

The sources and sinks in the carbon cycle do not participate in the cycle evenly for all isotopologues, which is due to fractionation. This is defined as the separation of lighter and heavier isotopes as a result of physical processes in the ecosystem having a (slight) preference for one. For example, the photosynthesis process in plants prefers carbon 12 over carbon 13 and thus results in an overall negative δ^{13} value, while water bodies take up heavier isotopes due to them having a higher probability of being closer to the bodies as they are heavier. Therefore, the importance of measuring the isotopic composition of carbon dioxide can be seen, as it helps identify sources and sinks in the surrounding environment that participate in the carbon cycle and allows us to target them in an effective way to reduce the emission in sources and increase uptake in sinks. In order to properly understand this process, the role of δ^{13} must be further observed.

The value of δ^{13} in the atmosphere experiences a seasonal variation. This is due to the fact that in winter, plants stop photosynthesizing and the main process governing the isotope ratios is respiration. This respiration brings the 13C isotope-depleted plant material back into the atmosphere, thereby decreasing the δ^{13} value overall. The opposite is the case during summer, when photosynthesis counters the uptake of carbon dioxide through respiration and also shows a preference for carbon 12, leaving a high concentration of carbon 13 in the atmosphere[12]. Therefore, it is evident that carbon 13 is very useful as a indicator of the strength of sinks present in the carbon cycle[12].

3 Instrumentation

3.1 IRMS

Isotope ratio mass spectrometry is the traditional method used to determine the isotopic composition of a sample. The IRMS requires a pure sample of CO_2 for measurement, which is the main argument against its effectiveness as a measurement method for atmospheric samples. At the CIO lab, the dual inlet IRMS is used, which takes measurements by alternating the aliquots of the pure CO_2 with a standard gas which allows for the δ^{13} and δ^{18} values to be measured due to the determined ratios. An advantage of using this method is that since the IRMS measures relative isotopic abundance compared to a standard gas, this compensates for any corrections that may need to be made due to sample evolution with time when measuring absolute ratios[13]. The IRMS functions very similarly to a conventional mass spectrometer but over a much narrower range of masses, allowing for a greater precision[13]. The diagram below illustrates the spectrometry method.

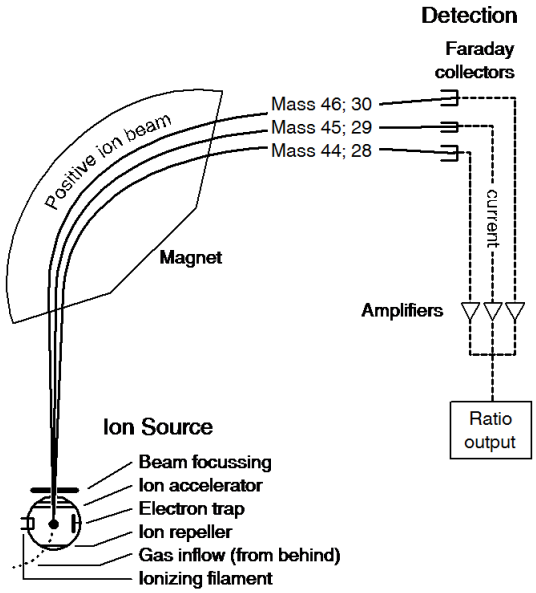

Figure 2: Diagram of an isotope ratio mass spectrometer.

The sample is initially ionized and the resulting beam of ions is directed towards the magnetic field created by the electromagnets. Due to their charge, the ions experience the Lorentz force which causes their trajectory to deviate depending upon their mass to charge ratio, allowing for separation of the isotopologues. These resulting beams are then collected by Faraday cups and are digitised and the resulting data is analyzed to determine the relative isotopic abundances.

The main drawback of using this method is that the sample preparation is very time consuming due to the fact that atmospheric samples need to have the CO_2 extracted out of them and then dried in order to make them acceptable to be measured by the machine.

3.2 SICAS

The Stable Isotope CO_2 Absorption Spectrometer(SICAS) offers one major advantage over the IRMS, which is the reduction in preparation time for samples. For atmospheric samples to be

measured by the IRMS, a pure CO_2 sample is required, which is time consuming and can lead to human errors being introduced into the measurement. Since the samples are directly measured after being collected for the SICAS, the risk of any fractionation effects due to present moisture is very low, improving the accuracy of the measurement process for atmospheric samples.

However, due to the absorption line fit not being exact, the mole fraction of CO_2 gas in the sample can influence the ratio of stable isotopes, thus requiring calibration in order to correct as much as possible[8]. There are two methods that can be used to carry this out, namely the isotopologue method and ratio method. The former requires calibration of the isotopologue fractions of CO_2 separately and using this to calculate their ratios, while the latter is very similar to the IRMS, in which the isotopologue ratios are determined first against a standard, and then calibrated to correct the values. This thesis will also try and determine which method performs better when using reference calcites. Diagrams of the optical board of the SICAS and the inlet system are shown below.

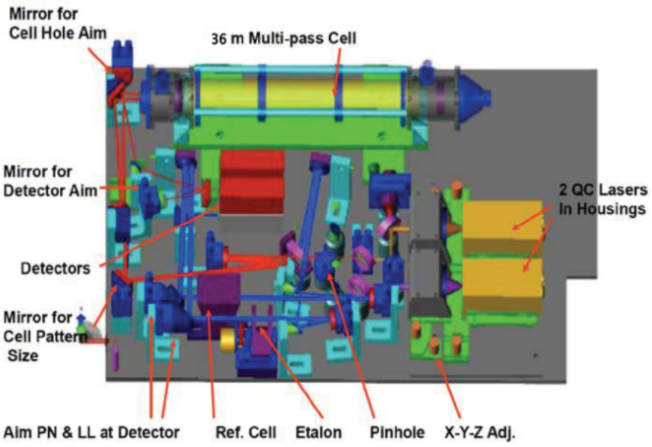

Figure 3: Optical board of SICAS[8]

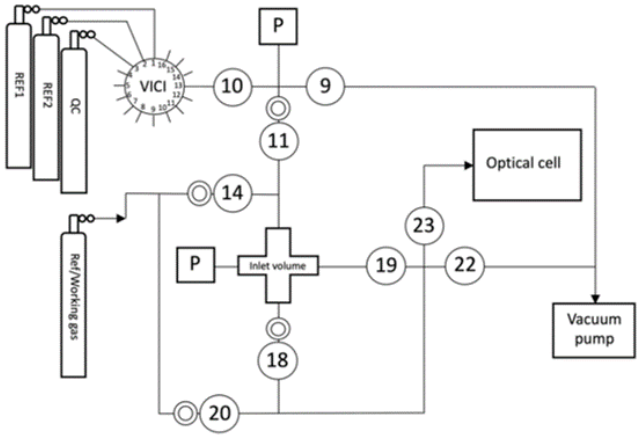

Figure 4: Gas inlet system SICAS

The optical board of the SICAS is designed with two lasers which operate over different spectral ranges to allow all the stable isotopologues of CO_2 to be detected. The laser beams are cooled and stabilized, after which they are passed through a cell containing the air sample to be measured. The entire system is flushed with nitrogen to ensure that only the absorption spectra of CO_2 from the air sample are detected, and the beams make their way to the infra-red detector, which digitises and stores the signal. Fitting the signal measured against a database of known molecular profiles can then be performed[8]. This information is then used to calculate the the isotopologue ratios.

The mechanical system that makes up the SICAS is shown on the right, and is completely controlled by the TDLWintel software through the use of scripts written for the measurement process. The reference and quality control tanks are used in a similiar method to the IRMS to calculate the isotopologue ratios and consequently the delta values. Multiple flasks can be connected to the VICI ports, and the valves in the system are designed to prevent cross contamination between the samples through the use of a vacuum pump. The measurements of samples is carried out in the optical cell, which can be completely isolated from the rest of the system. This allows the rest of the system to be flushed and vacuumed to prepare the next sample to measure while the current sample is being measured. Initially, a sample is let into the

inlet volume, where it is pressurized to a value of 200 mbar. From here the valves to the optical cell are opened once it has been vacuumed out, thus making the sample pressure inside the cell to be around 50 mbar. Since the entire process is controlled by the TDLWintel software, the time valves are open can be exactly controlled depending on pressure to ensure exactly the right amount of sample passes through. This aliquot is then measured and the cell is evacuated for the next measurement. The reference tanks are regularly measured in between sample measurements to determine the ratios. For each sample, a total of 9 aliquots are collected, and the data for all of them is combined into a single measurement set after any outliers have been removed.

The reference tanks have varying CO_2 concentrations from 350 ppm to around 440 ppm, along with varying delta values for 13C, 18O and δ^{17}. This is to ensure that the sample being measured falls within this range to allow for its isotope ratios to be accordingly fitted. A linear and quadratic fit can be applied to the data and both methods will be further analyzed to determine the more accurate method.

4 Experimental Method

4.1 Extraction of Carbon Dioxide

The extraction of carbon dioxide begins with weighing out the amount of calcite required to produce a vial that has a pressure no less than 150 mbar, as this is the minimum calculated pressure which allows for both a collection of five sample flasks with atmospheric concentration, and measurement by the IRMS. This sample is then isolated into a vial which allows for the calcite to be kept separate from the over saturated phosphoric acid, which is added into the vial next. This prevents any H20 forming in the subsequent reaction with the acid and calcite to react with the CO_2 formed. In order to ensure that there is no moisture in the vial, phosphorus pentoxide is added to the acid, as it is a drying agent. It works by reacting with any moisture in the vial to produce phosphoric acid, thus reducing the risk of δ^{18} contamination due an exchange of oxygen isotopes in the presence of water. This reaction is exothermic and thus the vial is kept in a water bath at a controlled temperature of 25°C and left for at least an hour to allow the temperature to equilibrate and any remaining moisture in the vial to react with the drying agent. The acid is then mixed with the calcite to produce carbon dioxide and left for a minimum period of 12 hours to allow the reaction to completely terminate and for maximum CO_2 to be extracted. The accumulated gas in the tube is then transferred with the help of cryo trapping into a different vial, at which point the vial is ready to use after a brief homogenization period.

In order to test the reliability of the dilution setup and become familiar with it, the experiment was first carried out using local gas references that were created in the laboratory, namely GS-19 and GS-20. Once this was achieved, five reference calcites were processed to create ten vials to be used by the dilution setup. Three samples were collected from each vial and using the insight from the results the experiment was repeated with two calcites with five vials created for each. Five samples were then created per vial using the dilution setup for a total data set of 50 potential samples to be used in the analysis and comparison. Initially the large range of the isotope values of δ^{13} and δ^{18} over the carbonate samples allowed for a broad testing of the SICAS over the range. However, when using just two calcites, one calcite (MAR-J1) was chosen as it had similar values to the target tanks, while the other (USGS-44) has isotope values on the other end of the spectrum.

4.2 Setup

The setup shown above is used to dilute the pure carbon dioxide samples from the vials to a concentration of 400 parts per million(ppm). The setup consists of a dilutor gas, which is composed of natural air pressurized in the cylinder. This air is led through an ascarite scrubber to remove carbon dioxide and magnesium perchlorate acting as a dryer by removing moisture. A mass flow controller(MFC) is in the line to ensure that the flow is such that the scrubbing processes are efficient.

The calibrated volumes are present right next to the flask and have a connection point beneath where the vial with a pure CO_2 sample is attached. The black strips represent an adjustable volume which can be increased or decreased by twisting to obtain the required pressure. The valves right above the adjustable volume separate two regions directly connected to the pressure sensor that are calibrated. The region directly next to the sensor has a volume of 2.3 ml while the region isolated by the valves has a volume of 1.5 ml to make a combined volume of 3.8 ml. Determining the pressure in these calibrated regions allows for the volume of the CO_2

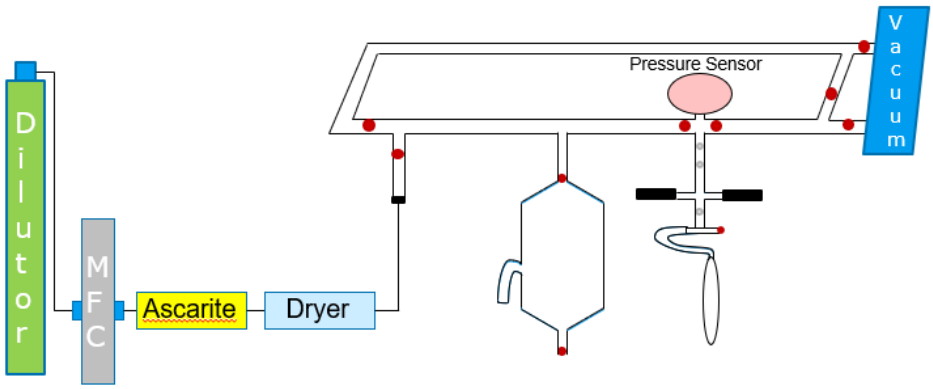

Figure 5: Dilution setup. Grey and red dot signify valves

calculated, which is crucial in making sure that the final volume of the flask is within the required bounds(more than 700 millibar and less than 1500 millibar).

Finally, a vacuum pump is connected to the end of the setup, its primary purpose being to evacuate different parts of the system to ensure that no cross contamination with lab air occurs. The red dots on the diagram indicate valves present in the system while the grey dots represent the valves present in the calibrating volume.

4.3 Dilution process

The dilution process is broken down into 5 steps which are all followed in chronological order to obtain a finished sample.

- First the flask, and the vial containing pure CO_2 are attached to their respective connection points and evacuation of the flask and calibration system is carried out.
- Once the minimum pressure of 1.33E-5 bar, which is the lowest possible pressure to measure with the sensor, has been reached, the calibration volumes are isolated from the rest of the system by closing the valves on either side of the pressure sensor.
- The pure CO_2 can then be let into the system. A vial of pure CO_2 with a pressure of around 170 millibar can produce at least 5 samples and so it is imperative to transfer the sample in batches to ensure minimal sample waste occurs due to evacuation between samples. First the valve right next to the vial is closed and the vial is opened and left for a period of 1 minute to ensure no isotope fractionation occurs. Then the vial is closed, preserving most of the sample. The valve can then be opened to the calibrated volumes and using the variable volume the pressure can be adjusted to ensure that the CO_2 concentration in the final sample will be close to 400 ppm.

  The following formula is used to calculate the pressure required for the samples. V_f stands for the volume of the flask and P represents the target pressure of the final sample. C is the value of the end CO_2 concentration of the sample, which for this experiment is taken to be a constant at 400 ppm. Finally, V_cal stands for the value of the calibrated volume. The formula can then be manipulated to get the sample pressure when all the other values are

determined. In essence, the equation is a modified version of the pressure volume formula, which states that the product of the pressure and volume in a closed system are constant.

$$Pressure = ((V_f * P) * C)/V_{cal} \quad (2)$$

In order for the SICAS to carry out its entire measurement sequence, a minimum sample pressure of 700 millibar is required and so the lower bound for the sample pressure for the purpose of this experiment was set to be 750 millibar. Dilution of the CO_2 to 400 ppm is carried out because the SICAS has been developed to measure samples with atmospheric concentration.

- Once the sample pressure has been determined using either or both calibrated volumes, the CO_2 can be transferred to the flask and frozen in the finger with the help of liquid nitrogen. First a reservoir is filled with liquid nitrogen and the tip of the finger is cooled before the CO_2 is introduced into the flask. Once the liquid nitrogen stops rapidly bubbling, the valve can be opened and due to the comparatively high sublimation temperature($-78.5°C$) of the CO_2 compared to the liquid nitrogen($-196°C$), the CO_2 will sublimate onto the walls of the freezing finger. While this process is occurring, the reservoir should be slowly moved up over the course of 4 minutes to surround as much of the freezing finger as possible by liquid nitrogen. This process is used to ensure the maximum amount of CO_2 gets trapped due to the slow periodic upward motion cooling the finger in stages and allowing for more exposure.

- The dilutor gas is then let into the system just as the reservoir of liquid nitrogen is removed. This is done to ensure the sample stays trapped in the flask. The liquid nitrogen reservoir is removed to ensure that the CO_2 free air entering the flask does not change its state and thus provides an accurate pressure reading on the sensor. The flask is brought up to the required pressure and then closed and set aside for a period of at least 12 hours to allow the sample inside to completely homogenize.

In addition to the steps above, there are a few more steps that were taken in order to ensure consistency in results and to identify any collected samples which may have been contaminated and remove them from the final results. This process also reduces the human error which is always present in the creation of the sample due to the dilution process and the creating of the pure samples. The freezing time for the transfer of CO_2 into the finger was always kept at a constant at 4 minutes. The scrubber and dryer were regularly checked to ensure that they were performing optimally. The mass flow controller was set to a output value of 0.3 liters per minute, much lower than the highest acceptable value of 0.45 liters per minute. This ensures that the dilutor gas is as CO_2 and H2O free as possible. After the transfer of CO_2 to the freezing finger was complete, the flask was opened to the vacuum briefly with the liquid nitrogen reservoir still present around the finger. Since the system was completely vacuumated prior to the transfer, any impurities in the pure CO_2 would be detected by a slight increase in the pressure and this not only allows the sample to be flagged but also removes the impurities so creates a greater chance that the sample may still be usable in the results. Due to the nature of the rotating valves used in the system, when using both calibrated volumes(which was the case for the majority of the samples) the exact volume could not be determined. Therefore, a rule of opening the valve only until the pressure equalized was implemented, which allowed the real pressure to be as close to the expected calibrated pressure as possible. With all of these implemented, the quality of the sample collected meets the standard in an experiment which requires constant human input.

4.4 SICAS

When the samples have been allowed to homogenize for the determined period of time, they are attached to the ports of the SICAS. Initially, before the measurement process starts, the port system and the tubes connecting the VICI ports to the flasks is put through a leak testing program to catch and allow manual fixing of any potential anomalies. Once this data is satisfactory, the measurement program can be started and the flasks opened to allow the sample into the machine. Due to regular flushing with the reference and target tanks, the risk of cross contamination between samples in minimal and so all flasks can be opened simultaneously provided that the VICI ports are functioning properly. Nine aliquots of sample are collected from each flask and measured by the machine and the data is logged into a STR and STC file format. One flask takes approximately two hours to be completely measured. Once the measurement cycle is complete and all flasks have been measured, the STR and STC files can be taken and run through an R program created to analyze the data, where it converts it into an Excel spreadsheet. During this process, corrections to the data are applied and any outliers are removed from the presented data. The SICAS can provide data for the ratio and isotopologue method simultaneously in one measurement which makes them easy to compare. For each individual method, the linear and quadratic fit are applied. Detailed descriptions of these methods can be found in the paper by P.M. Steur[8]. The data is then tabulated and can be seen in the section below.

4.5 IRMS

The measurement process with the IRMS involves taking the vial of pure CO_2, and transferring its contents to the bellow of the IRMS. The volume of the bellow is around 50 milliliters, and for optimal measurement a pressure between 5 to 7 millibars is desirable. The sample is ionized and the beam flowing towards the faraday cups is adjusted to obtain a current close to 4nA. The machine then takes 8 aliquots from the vial and measures them against a reference gas alternately, providing the isotopologue ratios as a result.

5 Results and Discussion

The results for the first five reference calcites, namely IAEA-603, NBS-19, NBS-18, MAR-J1 and HGJC were first collected. NBS-19 is the former international calibration material for the VPDB scale, succeeded by IAEA-603. NBS-18 is international reference material while MAR-J1 is the local reference material from Jena. Finally, HGJC is a local reference material for the CIO. Their values are included in the appendix. For these results, the isotopologue method and ratio method were compared to see which method provided more accuracy. On top of this, the data was also analyzed using a linear and a quadratic fit to see which fit performed best. The values of δ^{13} and δ^{18} were compared to the assigned values of the calcites. This allows for the residuals to be determined and a comparison between the IRMS and SICAS to be made. The averaged results are presented in the tables below but the full set can be found in the appendix. Residuals are calculated as measured minus assigned values.

Date	**CoK no**	**sample**	δ^{13} **residual**	δ^{18} **residual**	**IRMS** δ^{13} **residual**	**IRMS** δ^{18} **residual**
20/05/2021	15845	IAEA-603	-0.164	-0.074	0.020	-0.348
21/05/2021	15846	IAEA-603	-0.166	-0.145	0.060	-0.257
20/05/2021	15847	NBS-19	-0.106	-0.029	0.109	-0.058
22/05/2021	15848	NBS-19	-0.140	-0.071	-0.136	-0.368
20/05/2021	15850	NBS-18	0.021	0.381	0.099	0.246
20/05/2021	15851	MARJ-1	-0.319	0.198	-0.124	-0.125
22/05/2021	15852	MARJ-1	-0.143	0.429	0.023	0.328
21/05/2021	15853	HGJC	0.918	-0.046	1.019	-0.119
22/05/2021	15854	HGJC	0.018	0.012	0.122	-0.173

Table 1: Initial Residual values linear ratio method

Date	**CoK no**	**sample**	δ^{13} **residual**	δ^{18} **residual**	**IRMS** δ^{13} **residual**	**IRMS** δ^{18} **residual**
20/05/2021	15845	IAEA-603	0.205	-0.022	0.021	-0.348
21/05/2021	15846	IAEA-603	0.211	-0.095	0.060	-0.257
20/05/2021	15847	NBS-19	0.256	0.031	0.109	-0.058
22/05/2021	15848	NBS-19	0.199	-0.022	-0.135	-0.368
20/05/2021	15850	NBS-18	0.181	0.204	0.099	0.246
20/05/2021	15851	MARJ-1	0.035	0.253	-0.123	-0.125
22/05/2021	15852	MARJ-1	0.193	0.476	0.023	0.328
21/05/2021	15853	HGJC	1.177	-0.121	1.019	-0.119
22/05/2021	15854	HGJC	0.179	-0.073	0.122	-0.173

Table 2: Initial Residual values linear isotopologue method

Date	**CoK no**	**sample**	δ^{13} **residual**	δ^{18} **residual**	**IRMS** δ^{13} **residual**	**IRMS** δ^{18} **residual**
20/05/2021	15845	IAEA-603	-0.089	-0.014	0.021	-0.348
21/05/2021	15846	IAEA-603	-0.089	-0.071	0.060	-0.257
20/05/2021	15847	NBS-19	-0.032	0.024	0.109	-0.058
22/05/2021	15848	NBS-19	-0.052	0.025	-0.136	-0.368
20/05/2021	15850	NBS-18	0.062	0.411	0.099	0.246
20/05/2021	15851	MARJ-1	-0.245	0.252	-0.124	-0.125
22/05/2021	15852	MARJ-1	-0.057	0.522	0.023	0.328
21/05/2021	15853	HGJC	0.994	0.028	1.019	-0.119
22/05/2021	15854	HGJC	0.069	0.066	0.122	-0.173

Table 3: Initial Residual values quadratic ratio method

Date	CoK no	sample	δ^{13} residual	δ^{18} residual	IRMS δ^{13} residual	IRMS δ^{18} residual
20/05/2021	15845	IAEA-603	0.140	0.010	0.021	-0.348
21/05/2021	15846	IAEA-603	0.126	-0.052	0.060	-0.257
20/05/2021	15847	NBS-19	0.187	0.057	0.109	-0.058
22/05/2021	15848	NBS-19	0.182	0.053	-0.136	-0.368
20/05/2021	15850	NBS-18	0.149	0.206	0.099	0.246
20/05/2021	15851	MARJ-1	-0.027	0.279	-0.124	-0.125
22/05/2021	15852	MARJ-1	0.177	0.552	0.023	0.328
21/05/2021	15853	HGJC	1.091	-0.075	1.019	-0.119
22/05/2021	15854	HGJC	0.174	-0.039	0.122	-0.173

Table 4: Initial Residual values quadratic isotopologue method

From the tables above, it is clear that the quadratic approach provides results that conform better to the experimentally determined values of the calcites. Therefore, for the second dilution experiments, only the quadratic fit will be applied to the collected data. For the purpose of this experiment, we have chosen a deviation in the residuals of 0.1 per mil to be an acceptable range. The data collected can be summarized by observing that the quadratic fit using the ratio method performs the best, with seven out of nine samples having a δ^{13} residual value within the acceptable range while six out of nine samples had the same for δ^{18}. However, due to the fact that multiple different calcites were used, the results must be accepted with caution due a relative lack of repeatability and a high possibility of inaccuracies being introduced into the results due to a high human error possibility in sample preparation. Therefore, the experiment is repeated with five vials of two calcites each. These calcites are MAR-J1 and USGS-44. The results are summarized below.

Date	CoK no	sample	δ^{13} residual	δ^{18} residual	IRMS δ^{13} residual	IRMS δ^{18} residual
24/06/2021	15887	MAR-J1	-0,241	0,287	0,014	0,095
25/06/2021	15888	MAR-J1	-0,222	0,332	0,042	0,126
28/06/2021	15890	MAR-J1	-0,209	0,436	-0,158	0,215
30/06/2021	15889	MAR-J1	-0,190	0,383	0,023	0,197
01/07/2021	15891	MAR-J1	-0,318	0,136	0,013	0,160
24/06/2021	15892	USGS-44	1,053	0,151	0,400	-0,188
26/06/2021	15893	USGS-44	1,096	0,151	0,352	-0,166
29/06/2021	15895	USGS-44	1,074	0,202	0,525	-0,043
01/07/2021	15894	USGS-44	1,088	0,241	0,295	-0,077
02/07/2021	15896	USGS-44	1,041	0,106	0,362	-0,161

Table 5: Final Residual values ratio method

Date	CoK no	sample	δ^{13} residual	δ^{18} residual	IRMS δ^{13} residual	IRMS δ^{18} residual
24/06/2021	15887	MAR-J1	0.014	0.317	0.014	0.095
25/06/2021	15888	MAR-J1	0.027	0.379	0.042	0.126
28/06/2021	15890	MAR-J1	0.042	0.455	-0.158	0.216
30/06/2021	15889	MAR-J1	0.075	0.425	0.024	0.198
01/07/2021	15891	MAR-J1	-0.058	0.150	0.013	0.161
24/06/2021	15892	USGS-44	0.272	0.006	0.400	-0.188
26/06/2021	15893	USGS-44	0.352	0.033	0.353	-0.166
29/06/2021	15895	USGS-44	0.270	0.038	0.526	-0.043
01/07/2021	15894	USGS-44	0.365	0.114	0.295	-0.078
02/07/2021	15896	USGS-44	0.249	-0.063	0.362	-0.161

Table 6: Final Residual values isotopologue method

If we look at the first experiment, we can gain a better understanding of the system and understand why the secondary set of results has been collected. Firstly, the difference between using the linear and quadratic analysis method is very evident in the values of the residuals for δ^{13} and δ^{18}. The fractionation process can cause some deviations in the δ^{18} value of the sample when it has come in contact with any moisture during the preparation process, and so the δ^{13} residual values in this case are more reliable to make assumptions and draw conclusions from. The linear method clearly shows more inconsistency in the isotope values, reflected in the fact that for δ^{13} there is only one acceptable residual value for the ratio method and two for the isotopologue. The quadratic method shows much more promise, with 7 acceptable residual values using the ratio method and one using the isotopologue method. The large difference between the ratio and isotopologue method can be accounted for by analysing the residuals to observe if a scale calibration issue is the root cause. This is done by taking the standard deviations of the residuals of all samples and observing how small the resulting values are. In general, the smaller the value, the more likely it is that the cause of this dissimilarity is the lack of calibration of the SICAS. However, due to a smaller data set of each calcite, the standard deviations of these residuals are not very insightful in helping us determine whether the high residuals are present due to human error in the preparation process, or a scale correction that needs to be made to the SICAS.

Secondly, the data set with five calcites also has a more inaccurate dilution process due to the lack of experience with the system. This results in more samples being contaminated and thus unavailable for use in the data set. There is also a higher variability in the CO_2 concentration for these samples, another factor that needs to be accounted for by the SICAS as the CO_2 concentration should fall between the upper and lower bounds set by the target tanks in order for the sample to be accurately measured via the ratio method. However this is a minor issue and can be eliminated by having more experience with the system.

One example of the optimization of the dilution process is when the cryo-freezing of the CO_2 into the flask finger was carried out by manually holding the liquid nitrogen filled styrofoam vessel with tongs for a duration of four minutes. Due to it being difficult to keep the vessel at a constant height for such a long duration, some of the CO_2 inevitably escaped and led to the high standard deviation in CO_2 concentration that is observed. For the next set of dilutions, the adapted procedure made use of a stand upon with the vessel was placed and the stand height was periodically increased over the duration of the freezing process to ensure that the maximum amount of CO_2 was trapped. Another example of optimization is the homogenization process when the vial was opened to the calibration system. Initially this process was carried out rather quickly and the vial closed promptly after the pressure equalized due to lack of knowledge. This might have resulted in isotope mass fractionation occurring, where the lighter particles present in the vial have a higher chance of being transported to the vacuum present in the calibration system. This leaves the isotopes with larger mass in the vial and can lead to discrepancies between the data collected for IRMS and SICAS or even between the samples themselves. This practice was corrected by letting the sample measured homogenize in the new volume for a minimum period of one minute before the vial was closed off again.

The number of samples collected per vial of pure CO_2 also determines the reliability of the measurements. As described above, the lower the sample number, the less reliable the residual analysis. This low sample count also affects the mean isotope values, as the standard deviation increases. With the addition of a suspect(contaminated) sample, the data available for the vial

becomes even smaller as the suspect sample is excluded from the final results. This reduces the overall accuracy of the data and thus requires another set of measurements to correct for these issues.

The secondary set of measurements for MAR-J1 and USGS-44 contain 25 sample flasks collected over five vials each, thus reducing the effects of the issues faced before when combined with the method optimization. Looking at the data initially, there is one main fact that stands out. The isotopic values of δ^{13} and δ^{18} for the MAR-J1 calcite can be seen to conform a lot more to the expected values in that the residuals are comparatively very small. This is due to the fact that the δ^{13} and δ^{18} values of MAR-J1 are relatively close to the values of the target tanks against which it is measured. In essence, this means that the SICAS is calibrated to accurately determine the composition of the MAR-J1 calcite. On the other end of the scale, the isotopic values for USGS-44 are on the opposite end of the spectrum and thus cannot be accurately determined by the SICAS due to the target tank values not being close to calcites composition. However, while the δ^{13} and δ^{18} values for USGS-44 might not be accurate, they are still precise and depending on the value of the standard deviation can tell us whether this is due to calibration issues or human error, as described above. The standard deviations of the residuals using the isotopologue and ratio method are summarized in the table below. Some samples have been removed from this calculation due to their standard deviations not conforming with the rest of the group.

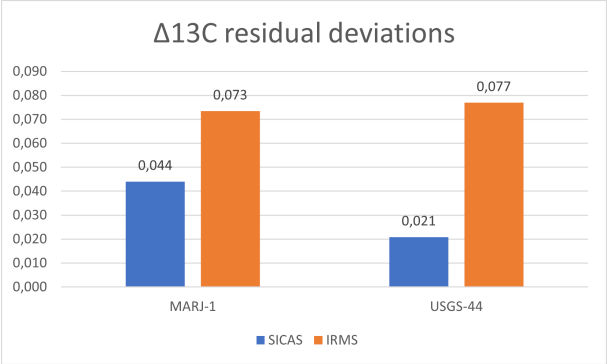

Figure 6: Residual deviations for δ^{13} using ratio method

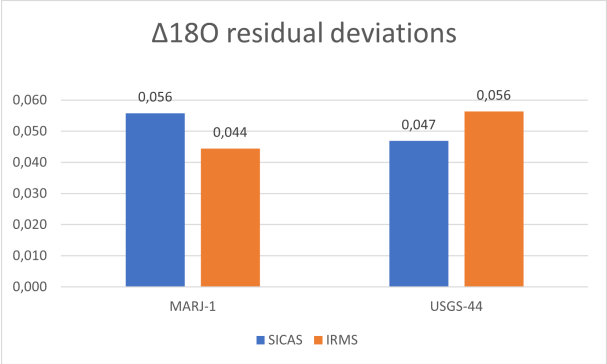

Figure 7: Residual deviations for δ^{18} using ratio method

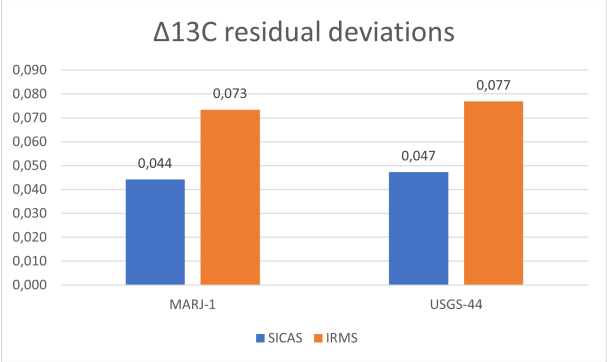

Figure 8: Residual deviations for δ^{13} using isotopologue method

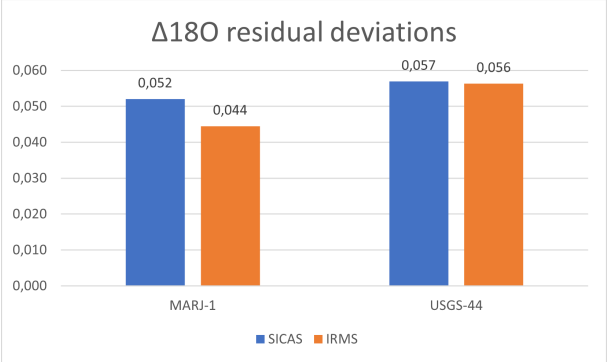

Figure 9: Residual deviations for δ^{18} using isotopologue method

First, when looking at the differences in the tabular data between the ratio and isotopologue method, it may seem that the isotopologue method is better in this case as for the MAR-J1 every vial had a mean δ^{13} residual value less than 0.1 while the opposite was the true for USGS-44. However, when the standard deviations of the residuals are analyzed, it can be seen that the difference between the two methods is minimal and the discrepancy is caused mainly due to calibration effects in the SICAS. When compared to the IRMS, the values can be observed to be relatively similar. Graphically, it is observed that the precision of the measurements for δ^{18} is constant across both the SICAS and the IRMS. The SICAS can be seen to have slightly better precision when it comes to measuring δ^{13}, which can be attributed to it being a newer setup that benefits from a higher level of precision. Therefore we can come to the conclusion that when the sample is prepared with a high enough accuracy and precautions are taken to ensure that there is no contamination in the dilution process, the IRMS and SICAS perform with a matching level of precision.

The storage of the pure CO_2 samples in the vials was also a concern during the dilution process, as the IRMS required a pure sample to measure while the SICAS required samples diluted to atmospheric concentrations. In order to observe and analyze this issue, the entire batch of vials was divided into two groups, one which was measured by the IRMS first and the other which was diluted and measured by the SICAS first. This was mainly done to see if the dilution setup produced any effects on the δ^{13} and δ^{18} values of the remaining CO_2 in the vials. The ID for vials which were measured by the IRMS first are 15890, 15891, 15895 and 15896. The rest of the vials were used to dilute 5 flasks to atmospheric CO_2 concentration and then

measured by the IRMS. After removing all outliers, the mean residual standard deviations are summarized in the table below.

	δ^{13} **residual** σ	δ^{18} **residual** σ	**IRMS** δ^{13} **residual** σ	**IRMS** δ^{18} **residual** σ
IRMS first	0.0502	0.048	0.086	0.028
Dilution first	0.026	0.045	0.012	0.043

Table 7: MAR-J1 comparison

	δ^{13} **residual** σ	δ^{18} **residual** σ	**IRMS** δ^{13} **residual** σ	**IRMS** δ^{18} **residual** σ
IRMS first	0.011	0.050	0.082	0.059
Dilution first	0.041	0.046	0.043	0.048

Table 8: USGS-44 comparison

As can be observed for both sets of data, the standard deviations themselves are very small regardless of whether the vial was measured by the IRMS first or used to dilute the samples. There is some variation but that is well within the margin of error that can be expected for this experiment and thus it can be concluded that the effect of using the vial to dilute aliquots of CO_2 has no discernable effect on the overall composition of the sample present in the vial. This is to be expected as even during the dilution process, the vial only comes in contact with the calibration system which is brought to the lowest possible pressure (1.33e-5 bar) and so the risk of contamination is minimal and only exists at the point of contact, which would be the O ring seal or the valve that opens and closes the vial itself. This also works to reduce fractionation effects in the setup.

For the CO_2 that passes through the dilution setup, there is still the possibility of human error affecting the isotopic composition. The entire dilution system is constructed with glass tubes, and so the physical phenomena of adsorption could also potentially play a role. As the system needs to be repeatedly exposed to the lab air to change flasks and collect a new sample, the glass setup is exposed to the moisture in the air, which can adhere itself to the glass through adsorption and consequently affect the value of δ^{18} due to an isotopic exchange occurring. This experiment would be able to detect this if it were occurring on a relatively large scale, with the effect being a high value of the residual itself for δ^{18}. However, looking at the standard deviations we cannot make any statements in this regard due to both values being relatively similar and small. Therefore, this part of the experiment can be used to conclude that the dilution setup does not alter the isotopic composition of the sample and also protects the remainder of the original sample in the vial from being affected.

It has to be taken into account that even though the dilution setup has been proven to be an effective method to use while preparing samples for the SICAS, the human error still remains unpredictable and significant and should always be considered when handling data of this nature. The SICAS is a device built to measure atmospheric samples which do not require any processing, and thus the isotopic values of the carbonates used are most likely not in the range that it is expected to measure. However, the only method currently available to calibrate the device is through the preparation of a reference carbonate sample diluted to an atmospheric concentration. Therefore, this process must be carried out with the largest emphasis being put on the accuracy with which the samples are created to ensure that all future samples measured by the SICAS are measured on the correct calibrated scale.

6 Conclusion

This research outlined the method which is used by the IRMS and SICAS in order to obtain measurements from samples for their isotopic values, and made a comparison between numerous different methods used to analyze the collected data along with testing the validity of the dilution system. A preliminary set of measurements allowed for a comparison between the linear and quadratic fitting methods. Further testing with a smaller set of calcites and a larger number of samples allowed us to come to the conclusion that the ratio and isotopologue method work equally well, but sometimes suffer from an offset in their values due to calibration issues. Testing the validity of the dilution setup produced a successful result indicating that the setup does not alter the composition of the sample. Finally, when making a comparison between the IRMS and SICAS, we can say that they are both equally accurate and the nature of the sample determines which method is best suited to its measurement.

7 Further research

By using the dilution method in this experiment, we can summarize that the method does not have a significant contribution to the systematic errors present in the collection and measurement of a sample. Therefore, the dilution setup has been modified following in order to perform a similar function of diluting the samples of pure CO_2 that have been collected over the amazon rainforest by the ASICA project over the time period of 2016 to 2018. The samples have been collected over different altitudes and different regions by flights and then converted to a pure CO_2 sample and flame sealed for preservation in the laboratories.

There were several challenges that needed to be overcome to optimize the dilution setup from the previous configuration used for this thesis into its current one. First, a cracker was designed and calibrated to contain the sample and allow for a controlled break of the glass tubes in which the sample is contained. A water trap using ethanol and dry ice is installed right after in order to make sure the sample is as dry as possible. Finally, a calibrated volume needed to be installed after the water trap to make sure the exact amount of CO_2 in the sample can be measured to allow it to be diluted to a concentration of 400 ppm. An inventory of 1500 samples is available for measurement, of which so far 42 have been measured with the SICAS after dilution. Alls samples must be processed in the next calendar year, partly by the present method, and partly using the new IRMS machine which will arrive at the CIO January/February 2022.

References

[1] H. Shaftel, *Carbon dioxide — vital signs – climate change: Vital signs of the planet*, `https://climate.nasa.gov/vital-signs/carbon-dioxide/`, (Accessed on 09/04/2021), Sep. 2021.

[2] J. Melillo, T. Callaghan, F. Woodward, E. Salati, and S. Sinha, "Effects on ecosystems," *Climate change: The IPCC scientific assessment*, pp. 283–310, 1990.

[3] D. A. Lashof and D. R. Ahuja, "Relative contributions of greenhouse gas emissions to global warming," *Nature*, vol. 344, no. 6266, pp. 529–531, 1990.

[4] W. Peters, *Periodic reporting for period 3 - asica (new constraints on the amazonian carbon balance from airborne observations of the stable isotopes of co2) — report summary — asica — h2020 — cordis — european commission*, `https://cordis.europa.eu/project/id/649087/reporting`, (Accessed on 09/04/2021), 2014.

[5] M. Tiwari, A. K. Singh, and D. K. Sinha, "Stable isotopes: Tools for understanding past climatic conditions and their applications in chemostratigraphy," in *Chemostratigraphy*, Elsevier, 2015, pp. 65–92.

[6] S. Sakai, S. Matsuda, T. Hikida, A. Shimono, J. B. McManus, M. Zahniser, D. Nelson, D. L. Dettman, D. Yang, and N. Ohkouchi, "High-precision simultaneous 18o/16o, 13c/12c, and 17o/16o analyses for microgram quantities of caco3 by tunable infrared laser absorption spectroscopy," *Analytical chemistry*, vol. 89, no. 21, pp. 11 846–11 852, 2017.

[7] W. A. Brand, L. Huang, H. Mukai, A. Chivulescu, J. M. Richter, and M. Rothe, "How well do we know vpdb? variability of δ13c and δ18o in co2 generated from nbs19-calcite," *Rapid Communications in Mass Spectrometry: An International Journal Devoted to the Rapid Dissemination of Up-to-the-Minute Research in Mass Spectrometry*, vol. 23, no. 6, pp. 915–926, 2009.

[8] P. M. Steur, H. A. Scheeren, D. D. Nelson, J. B. McManus, and H. A. Meijer, "Simultaneous measurement of δ 13 c, δ 18 o and δ 17 o of atmospheric co 2–performance assessment of a dual-laser absorption spectrometer," *Atmospheric Measurement Techniques*, vol. 14, no. 6, pp. 4279–4304, 2021.

[9] S. M. Libes, "Blue planet: The role of the oceans in nutrient cycling, maintaining the atmospheric system, and modulating climate change," in *Routledge Handbook of Ocean Resources and Management*, Routledge, 2015, pp. 89–107.

[10] H. Riebeek, *The carbon cycle*, Jun. 2011. [Online]. Available: `https://earthobservatory.nasa.gov/features/CarbonCycle`.

[11] J. M. Hayes, "An introduction to isotopic calculations," *Woods Hole Oceanographic Institution, Woods Hole, MA*, vol. 2543, 2004.

[12] E. S. R. Laboratories, *Global monitoring laboratory - carbon cycle greenhouse gases*, `https://gml.noaa.gov/ccgg/isotopes/c13tellsus.html`, (Accessed on 10/17/2021).

[13] W. Meier-Augenstein, "Applied gas chromatography coupled to isotope ratio mass spectrometry," *Journal of Chromatography A*, vol. 842, no. 1-2, pp. 351–371, 1999.

8 Appendix

Reference Material	δ^{13}	δ^{18}
NBS-19	1.95‰	-2.20‰
NBS-18	-5.01‰	-23.2‰
IAEA-603	2.46‰	-2.37‰
HGJC	-4.28‰	-13.92‰
MAR-J1	1.96‰	-2.10‰
USGS-44	-42.21‰	-15.7‰

Table 9: Reference material delta values

Date	20/05/2021	21/05/2021	20/05/2021	22/05/2021	20/05/2021	20/05/2021	22/05/2021	21/05/2021	22/05/2021
CoK no	15845	15846	15847	15848	15850	15851	15852	15853	15854
sample	IAEA-603	IAEA-603	NBS-19	NBS-19	NBS-18	MARJ-1	MARJ-1	HGJC	HGJC
CO2 mean	385.66	376.95	382.06	387.68	397.48	386.36	388.24	375.55	399.29
CO2 stdev	4.94	1.47	7.66	3.41	23.14	3.36	6.49	3.06	20.38
δ^{13} **mean**	2.296	2.294	1.844	1.810	-4.993	1.640	1.817	-3.362	-4.261
δ^{13} **stdev**	0.0164	0.0302	0.0302	0.0139	0.0260	0.0280	0.0375	0.0284	0.0132
δ^{18}	-2.445	-2.516	-2.230	-2.271	-22.819	-2.382	-2.152	-13.966	-13.908
δ^{18} **stdev**	0.0202	0.0276	0.0200	0.0103	0.1355	0.0509	0.0318	0.0247	0.0259
IRMS δ^{13}	2.481	2.520	2.059	1.814	-4.914	1.836	1.983	-3.262	-4.158
error	0.0061	0.0079	0.0095	0.0065	0.0035	0.0100	0.0045	0.0082	0.0037
IRMS δ^{18}	-2.718	-2.627	-2.258	-2.568	-22.954	-2.705	-2.252	-14.039	-14.093
error	0.0049	0.0065	0.0080	0.0154	0.0081	0.0052	0.0078	0.0118	0.0186
δ^{13} **residual**	-0.1640	-0.1662	-0.1063	-0.1399	0.0207	-0.3197	-0.1435	0.9184	0.0189
δ^{18} **residual**	-0.0749	-0.1457	-0.0298	-0.0706	0.3813	0.1981	0.4285	-0.0455	0.0120
IRMS δ^{13} **residual**	0.0206	0.0602	0.1091	-0.1359	0.0999	-0.1238	0.0234	1.0185	0.1220
IRMS δ^{18} **residual**	-0.3483	-0.2571	-0.0577	-0.3682	0.2464	-0.1252	0.3279	-0.1187	-0.1731

Table 10: linear fit ratio method

Date	20/05/2021	21/05/2021	20/05/2021	22/05/2021	20/05/2021	20/05/2021	22/05/2021	21/05/2021	22/05/2021
CoK no	15845	15846	15847	15848	15850	15851	15852	15853	15854
sample	IAEA-603	IAEA-603	NBS-19	NBS-19	NBS-18	MARJ-1	MARJ-1	HGJC	HGJC
CO2 mean	385.64	376.93	382038.00	387.66	397.46	386.33	388.21	375.52	399.27
CO2 stdev	4.94	1.47	7.66	3.41	23.13	3.36	6.49	3.06	20.38
δ^{13} **mean**	2.665	2.671	2.206	2.150	-4.832	1.995	2.154	-3.103	-4.100
δ^{13} **stdev**	0.0206	0.0307	0.0360	0.0203	0.1117	0.0242	0.0530	0.0277	0.1038
δ^{18}	-2.392	-2.465	-2.169	-2.223	-22.996	-2.326	-2.104	-14.042	-13.993
δ^{18} **stdev**	0.0239	0.0278	0.0248	0.0122	0.1484	0.0532	0.0361	0.0233	0.0420
IRMS δ^{13}	2.481	2.520	2.059	1.814	-4.914	1.836	1.983	-3.262	-4.158
error	0.0061	0.0079	0.0095	0.0065	0.0035	0.0100	0.0045	0.0082	0.0037
IRMS δ^{18}	-2.718	-2.627	-2.258	-2.568	-22.954	-2.705	-2.252	-14.039	-14.093
error	0.0049	0.0065	0.0080	0.0154	0.0081	0.0052	0.0078	0.0118	0.0186
δ^{13} **residual**	0.2054	0.2113	0.2555	0.1996	0.1818	0.0354	0.1935	1.1772	0.1798
δ^{18} **residual**	-0.0219	-0.0954	0.0311	-0.0229	0.2036	0.2536	0.4765	-0.1215	-0.0733
IRMS δ^{13} **residual**	0.0206	0.0602	0.1091	-0.1359	0.0999	-0.1238	0.0234	1.0185	0.1220
IRMS δ^{18} **residual**	-0.3483	-0.2571	-0.0577	-0.3682	0.2464	-0.1252	0.3279	-0.1187	-0.1731

Table 11: linear fit isotopologue method

Date	20/05/2021	21/05/2021	20/05/2021	22/05/2021	20/05/2021	20/05/2021	22/05/2021	21/05/2021	22/05/2021
CoK no	15845	15846	15847	15848	15850	15851	15852	15853	15854
sample	IAEA-603	IAEA-603	NBS-19	NBS-19	NBS-18	MARJ-1	MARJ-1	HGJC	HGJC
CO2 mean	385.62	376.90	382.02	387.62	397.46	386.32	388.18	375.50	399.26
CO2 stdev	4.95	1.47	7.66	3.41	23.17	3.36	6.49	3.06	20.42
δ^{13} **mean**	2.371	2.370	1.918	1.899	-4.953	1.715	1.903	-3.286	-4.211
δ^{13} **stdev**	0.0171	0.0291	0.0303	0.0160	0.0726	0.0266	0.0438	0.0264	0.0743
δ^{18}	-2.384	-2.441	-2.176	-2.175	-22.789	-2.328	-2.058	-13.892	-13.854
δ^{18} **stdev**	0.0131	0.0272	0.0215	0.0128	0.1601	0.0517	0.0389	0.0226	0.0934
IRMS δ^{13}	2.481	2.520	2.059	1.814	-4.914	1.836	1.983	-3.262	-4.158
error	0.0061	0.0079	0.0095	0.0065	0.0035	0.0100	0.0045	0.0082	0.0037
IRMS δ^{18}	-2.718	-2.627	-2.258	-2.568	-22.954	-2.705	-2.252	-14.039	-14.093
error	0.0049	0.0065	0.0080	0.0154	0.0081	0.0052	0.0078	0.0118	0.0186
δ^{13} **residual**	-0.0887	-0.0898	-0.0320	-0.0515	0.0615	-0.2446	-0.057	0.9940	0.0688
δ^{18} **residual**	-0.0143	-0.0713	0.0238	0.0253	0.4108	0.2520	0.5225	0.028	66.0000
IRMS δ^{13} **residual**	0.0206	0.0602	0.1091	-0.1359	0.0999	-0.1238	0.0234	1.0185	0.1220
IRMS δ^{18} **residual**	-0.3483	-0.2571	-0.0577	-0.3682	0.2464	-0.1252	0.3279	-0.1187	-0.1731

Table 12: quadratic fit ratio method

Date	20/05/2021	21/05/2021	20/05/2021	22/05/2021	20/05/2021	20/05/2021	22/05/2021	21/05/2021	22/05/2021
CoK no	15845	15846	15847	15848	15850	15851	15852	15853	15854
sample	IAEA-603	IAEA-603	NBS-19	NBS-19	NBS-18	MARJ-1	MARJ-1	HGJC	HGJC
CO2 mean	385.60	376.87	381.99	387.60	397.43	386.29	388.15	375.47	399.24
CO2 stdev	4.95	1.47	7.66	3.41	23.17	3.36	6.49	3.06	20.42
δ^{13} **mean**	2.600	2.586	2.137	2.132	-4.865	1.933	2.137	-3.188	-4.106
δ^{13} **stdev**	0.0194	0.0292	0.0253	0.0150	0.0486	0.0300	0.0410	0.0267	0.0704
δ^{18}	-2.360	-2.422	-2.143	-2.147	-22.994	-2.300	-2.028	-13.995	-13.959
δ^{18} **stdev**	0.0170	0.0276	0.0255	0.0144	0.1723	0.0536	0.0424	0.0247	0.1040
IRMS δ^{13}	2.481	2.520	2.059	1.814	-4.914	1.836	1.983	-3.262	-4.158
error	0.0061	0.0079	0.0095	0.0065	0.0035	0.0100	0.0045	0.0082	0.0037
IRMS δ^{18}	-2.718	-2.627	-2.258	-2.568	-22.954	-2.705	-2.252	-14.039	-14.093
error	0.0049	0.0065	0.0080	0.0154	0.0081	0.0052	0.0078	0.0118	0.0186
δ^{13} **residual**	0.1404	0.1263	0.1872	0.1817	0.1494	-0.0273	0.177	1.0918	0.1737
δ^{18} **residual**	0.0101	-0.0515	0.0572	0.0534	0.2056	0.2799	0.552	-0.0745	-0.039
IRMS δ^{13} **residual**	0.0206	0.0602	0.1091	-0.1359	0.0999	-0.1238	0.0234	1.0185	0.1220
IRMS δ^{18} **residual**	-0.3483	-0.2571	-0.0577	-0.3682	0.2464	-0.1252	0.3279	-0.1187	-0.1731

Table 13: quadratic fit isotopologue method

Date	24/06/2021	25/06/2021	28/06/2021	30/06/2021	01/07/2021	24/06/2021	26/06/2021	29/06/2021	01/07/2021	02/07/2021
CoK no	15887	15888	15890	15889	15891	15892	15893	15895	15894	15896
sample	MAR-J1	MAR-J1	MAR-J1	MAR-J1	MAR-J1	USGS-44	USGS-44	USGS-44	USGS-44	USGS-44
CO2 mean	389.73	387.28	393.87	385.67	391.38	393.50	382.66	395.36	381.78	394.92
CO2 stdev	3.65	8.04	4.75	4.00	7.81	5.58	4.44	6.26	4.24	3.81
δ^{13} **mean**	1.719	1.738	1.750	1.770	1.641	-41.157	-41.113	-41.136	-41.121	-41.169
δ^{13} **stdev**	0.0180	0.0567	0.0635	0.0344	0.0393	0.0600	0.0412	0.0188	0.0063	0.0128
δ^{18}	-2.293	-2.247	-2.143	-2.196	-2.444	-15.549	-15.549	-15.497	-15.458	-15.594
δ^{18} **stdev**	0.0263	0.0525	0.0460	0.0357	0.0356	0.0736	0.0747	0.0873	0.0472	0.0596
IRMS δ^{13}	1.974	2.002	1.802	1.984	1.973	-41.810	-41.857	-41.684	-41.915	-41.848
IRMS δ^{18}	-2.485	-2.454	-2.364	-2.382	-2.419	-15.888	-15.866	-15.743	-15.778	-15.861
δ^{13} **residual**	-0.2412	-0.2222	-0.2097	-0.1903	-0.3189	1.0532	1.0966	1.0743	1.0886	1.0415
δ^{18} **residual**	-0.193	-0.147	-0.043	-0.096	-0.343	0.151	0.1512	0.2027	0.2418	0.1064
IRMS δ^{13} **residual**	0.0143	0.0421	-0.1584	0.0236	0.0132	0.4001	0.3526	0.5255	0.2951	0.3622
IRMS δ^{18} **residual**	0.025	0.056	0.146	0.128	0.091	-0.1881	-0.1663	-0.0434	-0.0775	-0.1612

Table 14: final data ratio method

Date	24/06/2021	25/06/2021	28/06/2021	30/06/2021	01/07/2021	24/06/2021	26/06/2021	29/06/2021	01/07/2021	02/07/2021
CoK no	15887	15888	15890	15889	15891	15892	15893	15895	15894	15896
sample	MAR-J1	MAR-J1	MAR-J1	MAR-J1	MAR-J1	USGS-44	USGS-44	USGS-44	USGS-44	USGS-44
CO2 mean	389.71	387.26	393.85	385.65	391.36	393.48	382.64	395.34	381.75	394.90
CO2 stdev	3.65	8.04	4.75	4.00	7.81	5.58	4.44	6.26	4.24	3.81
δ^{13} **mean**	1.974	1.987	2.002	2.035	1.902	-41.939	-41.858	-41.940	-41.845	-41.961
δ^{13} **stdev**	0.0205	0.0710	0.0701	0.0340	0.0480	0.0554	0.0582	0.0286	0.0283	0.0282
δ^{18}	-2.263	-2.200	-2.125	-2.155	-2.430	-15.694	-15.667	-15.662	-15.586	-15.763
δ^{18} **stdev**	0.0257	0.0483	0.0480	0.0369	0.0400	0.0744	0.0797	0.0882	0.0513	0.0604
IRMS δ^{13}	1.974	2.002	1.802	1.984	1.973	-41.810	-41.857	-41.684	-41.915	-41.848
IRMS δ^{18}	-2.485	-2.454	-2.364	-2.382	-2.419	-15.888	-15.866	-15.743	-15.778	-15.861
δ^{13} **residual**	0.0141	0.0267	0.0421	0.0753	-0.0583	0.2715	0.3516	0.2703	0.3653	0.2489
δ^{18} **residual**	-0.163	-0.100	-0.025	-0.055	-0.330	0.0056	0.0334	0.0381	0.114	-0.0627
IRMS δ^{13} **residual**	0.0143	0.0421	-0.1584	0.0236	0.0132	0.4001	0.3526	0.5255	0.2951	0.3622
IRMS δ^{18} **residual**	-0.385	-0.354	-0.264	-0.282	-0.319	-0.1881	-0.1663	-0.0434	-0.0775	-0.1612

Table 15: final data isotopologue method